SECTION I

INTRODUCTION TO DIFFUSION MRI

CHAPTER

1

Introduction to Diffusion MR

Peter J. Basser and Evren Özarslan

OUTLINE

I. What is Diffusion?	**3**
II. Magnetic Resonance and Diffusion	**5**
A. From the MR Signal Attenuation to the Average Propagator	*8*
III. Diffusion in Neural Tissue	**8**
IV. Concluding Remarks	**9**
Acknowledgments	**9**
References	**9**

ABSTRACT

Developments in the last century have led to a better understanding of diffusion, the perpetual mixing of molecules caused by thermal motion. In this chapter, the basic principles governing the diffusion phenomenon and its measurement using magnetic resonance (MR) are reviewed. The concepts of the apparent diffusion coefficient and of the diffusion propagator as well as their MR measurements are introduced from basic principles. Finally, the influence of neural tissue microstructure on the diffusion-weighted MR signal is briefly discussed.

Keywords: Diffusion, magnetic resonance, MRI, DWI, propagator, anisotropy, diffusion tensor, q-space, apparent diffusion coefficient

I. WHAT IS DIFFUSION?

Diffusion is a mass transport process arising in nature, which results in molecular or particle mixing without requiring bulk motion. Diffusion should not be confused with convection or dispersion – other transport mechanisms that require bulk motion to carry particles from one place to another.

The excellent book by Howard Berg (1983) *Random Walks in Biology* describes a helpful Gedanken experiment that illustrates the diffusion phenomenon. Imagine carefully introducing a drop of colored fluorescent dye into a jar of water. Initially, the dye appears to remain concentrated at the point of release, but over time it spreads radially, in a spherically symmetric profile. This mixing process takes place without stirring or other bulk fluid motion. The physical law that explains this phenomenon is called Fick's first law (Fick, 1855a, b), which relates the diffusive flux to any concentration difference through the relationship

$$\mathbf{J} = -D\nabla C \tag{1.1}$$

 Copyright © 2009 Elsevier Inc. All rights reserved

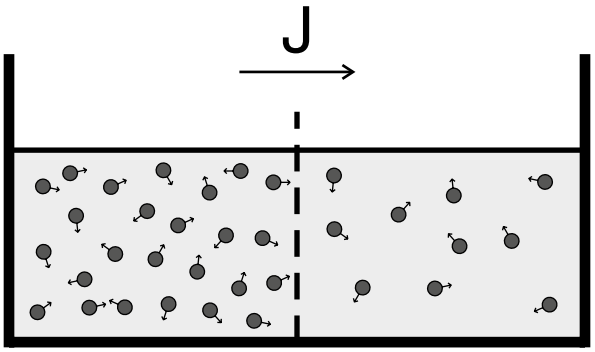

FIGURE 1.1 According to Fick's first law, when the specimen contains different regions with different concentrations of molecules, the particles will, on average, tend to move from high concentration regions to low concentration regions leading to a net flux (**J**).

where **J** is the net particle flux (vector), C is the particle concentration, and the constant of proportionality, D, is called the "diffusion coefficient". As illustrated in Figure 1.1, Fick's first law embodies the notion that particles flow from regions of high concentration to low concentration (thus the minus sign in equation (1.1)) in an entirely analogous way that heat flows from regions of high temperature to low temperature, as described in the earlier Fourier's law of heating on which Fick's law was based. In the case of diffusion, the rate of the flux is proportional to the concentration gradient as well as to the diffusion coefficient. Unlike the flux vector or the concentration, the diffusion coefficient is an intrinsic property of the medium, and its value is determined by the size of the diffusing molecules and the temperature and microstructural features of the environment. The sensitivity of the diffusion coefficient on the local microstructure enables its use as a probe of physical properties of biological tissue.

On a molecular level diffusive mixing results solely from collisions between atoms or molecules in the liquid or gas state. Another interesting feature of diffusion is that it occurs even in thermodynamic equilibrium, for example in a jar of water kept at a constant temperature and pressure. This is quite remarkable because the classical picture of diffusion, as expressed above in Fick's first law, implies that when the temperature or concentration gradients vanish, there is no net flux. There were many who held that diffusive mixing or energy transfer stopped at this point. We now know that although the net flux vanishes, microscopic motions of molecule still persist; it is just that on average, there is no net molecular flux in equilibrium.

A framework that explains this phenomenon has its origins in the observations of Robert Brown, who is

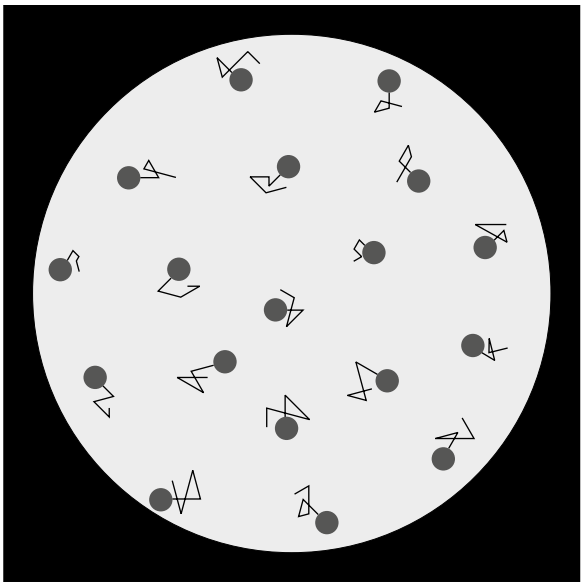

FIGURE 1.2 Robert Brown, a botanist working on the mechanisms of fertilization in flowering plants, noticed the perpetual motion of pollen grains suspended in water in 1827.

credited with being the first one to report the random motions of pollen grains while studying them under his microscope (Brown, 1828); his observation is illustrated in a cartoon in Figure 1.2. He reported that particles moved randomly without any apparent cause. Brown initially believed that there was some life force that was causing these motions, but disabused himself of this notion when he observed the same fluctuations when studying dust and other dead matter.

In the early part of the 20th century, Albert Einstein, who was unaware of Brown's observation and seeking evidence that would undoubtedly imply the existence of atoms, came to the conclusion that (Einstein, 1905; Fürth and Cowper, 1956) "…bodies of microscopically visible size suspended in a liquid will perform movements of such magnitude that they can be easily observed in a microscope". Einstein used a probabilistic framework to describe the motion of an ensemble of particles undergoing diffusion, which led to a coherent description of diffusion, reconciling the Fickian and Brownian pictures. He introduced the "displacement distribution" for this purpose, which quantifies the fraction of particles that will traverse a certain distance within a particular timeframe, or equivalently, the likelihood that a single given particle will undergo that displacement. For example, in free diffusion the displacement distribution is a Gaussian function whose width is determined by the diffusion coefficient as illustrated in Figure 1.3. Gaussian diffusion will be treated in more detail in Chapter 3,

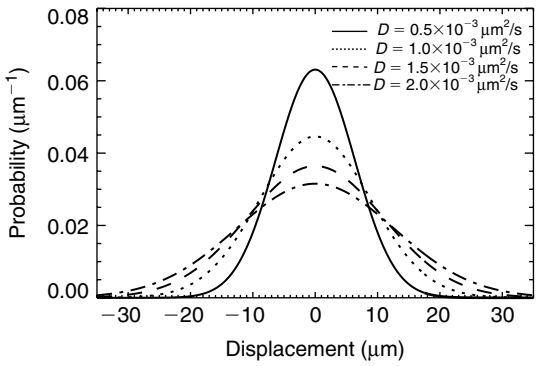

FIGURE 1.3 The Gaussian displacement distribution plotted for various values of the diffusion coefficient when the diffusion time was taken to be 40 ms. Larger diffusion coefficients lead to broader displacement probabilities suggesting increased diffusional mobility.

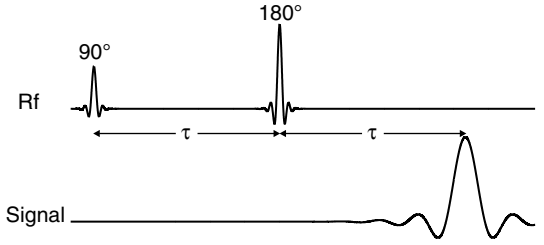

FIGURE 1.4 A schematic of the spin-echo method introduced by Hahn.

whereas the more general case of non-Gaussianity will be tackled in Chapters 4 and 7.

Using the displacement distribution concept, Einstein was able to derive an explicit relationship between the mean-squared displacement of the ensemble, characterizing its Brownian motion, and the classical diffusion coefficient, D, appearing in Fick's law (Einstein, 1905, 1926), given by

$$\langle x^2 \rangle = 2D\Delta \tag{1.2}$$

where $\langle x^2 \rangle$ is the mean-squared displacement of particles during a diffusion time, Δ, and D is the same classical diffusion coefficient appearing in Fick's first law above.

At around the same time as Einstein, Smoluchowski (1906) was able to reach the same conclusions using different means. Langevin improved upon Einstein's description of diffusion for ultra-short timescales in which there are few molecular collisions, but we are not able to probe this regime using MR diffusion measurements in water. Since a particle experiences about 10^{21} collisions every second in typical proton-rich solvents like water (Chandrasekhar, 1943), we generally do not concern ourselves with this correction in diffusion MR.

II. MAGNETIC RESONANCE AND DIFFUSION

Magnetic resonance provides a unique opportunity to quantify the diffusional characteristics of a wide range of specimens. Because diffusional processes are influenced by the geometrical structure of the environment, MR can be used to probe the structural environment non-invasively. This is particularly important in studies that involve biological samples in which the characteristic length of the boundaries influencing diffusion are typically so small that they cannot be resolved by conventional magnetic resonance imaging (MRI) techniques.

A typical nuclear magnetic resonance (NMR) scan starts with the excitation of the nuclei with a 90 degree radiofrequency (rf) pulse that tilts the magnetization vector into the plane whose normal is along the main magnetic field. The spins subsequently start to precess around the magnetic field – a phenomenon called Larmor precession. The angular frequency of this precession is given by

$$\omega = \gamma B \tag{1.3}$$

where B is the magnetic field that the spin is exposed to and γ is the gyromagnetic ratio – a constant specific to the nucleus under examination. In water, the hydrogen nucleus (i.e. the proton) has a gyromagnetic ratio value of approximately 2.68×10^8 rad/s/tesla. Spins that are initially coherent dephase due to factors such as magnetic field inhomogeneities and dipolar interactions (Abragam, 1961) leading to a decay of the voltage (signal) induced in the receiver.

As proposed by Edwin Hahn (Hahn, 1950), and illustrated in Figure 1.4, the dephasing due to magnetic field inhomogeneities can be reversed through a subsequent application of a 180 degree rf pulse, and the signal is reproduced. In this "spin-echo" experiment, the time between the first rf pulse and formation of the echo is called TE and it is twice the time between the two rf pulses, which is denoted by τ. The generated echo is detected by a receiver antenna (MR coil) and is used to produce spectra. Carefully devised sequences of rf pulses along with external magnetic field gradients linearly changing in space, enable the acquisition of magnetic resonance images. MR signal and image acquisition will be discussed in detail in Chapter 2.

The sensitivity of the spin-echo MR signal on molecular diffusion was recognized by Hahn. He reported a reduction of signal of the spin echo and explained it in terms of the dephasing of spins caused by translational diffusion within an inhomogeneous magnetic field (Hahn, 1950). While he proposed that one could measure the diffusion coefficient of a solution containing spin-labeled molecules, he did not propose a direct method for doing so.

A few years later, Carr and Purcell (1954) proposed a complete mathematical and physical framework for such a measurement using Hahn's NMR spin-echo sequence. They realized that the echo magnitude could be sensitized solely to the effects of random molecular spreading caused by diffusion in a way that permits a direct measurement. The idea they employed is not very different from what is utilized in most current studies of diffusion-weighted imaging. Because a spin's precession frequency is determined by the local magnetic field as implied by equation (1.3), if a "magnetic field gradient" is applied, spins that are at different locations experience different magnetic fields – hence they precess at different angular frequencies. After a certain time, the spins acquire different phase shifts depending on their location. Stronger gradients will lead to sharper phase changes across the specimen, yielding a higher sensitivity on diffusion. In most current clinical applications, a quantity called the "*b*-value", which is proportional to the square of the gradient strength, is used to characterize the level of the induced sensitivity on diffusion.

In the scheme considered by Carr and Purcell, a constant magnetic field gradient is applied throughout the entire Hahn spin-echo experiment as shown in Figure 1.5. Such an acquisition can be performed either in a spatially linear main field, or using another coil that is capable of creating a linear magnetic field on top of the homogeneous field of the scanner (B_0). In their description, at a particular time t, a particle situated at position x experiences a magnetic field of $B_0 + G\,x(t)$. If the particle is assumed to spend a short time, τ', at this point before moving to another location, it suffers a phase shift given by

$$\begin{aligned}\phi(x(t)) &= -\omega(x(t))\tau' \\ &= -\gamma(B_0 + G\,x(t))\tau'\end{aligned} \tag{1.4}$$

as a result of the Larmor precession at the field modified by the constant gradient. Here, the minus sign is necessary for protons whose precession is in the clockwise direction on the plane perpendicular to the main magnetic field. Therefore, the net phase shift that influences the MR signal at $t = 2\tau$ is related to the motional history of the particles in the ensemble. By exploiting this phenomenon Carr and Purcell proposed MR sequences to sensitize the MR spin echo to the effects of diffusion, and developed a rigorous mathematical framework to measure the diffusion coefficient from such sequences. This elevated NMR as a "gold standard" for measuring molecular diffusion. An alternative mathematical formulation of the problem was introduced by Torrey (1956) who generalized the phenomenological Bloch equations (Bloch, 1946) to include the effects of diffusion.

After about a decade, Stejskal and Tanner (1965) introduced many innovations that made modern diffusion measurements by NMR and MRI possible. First, they introduced the pulsed gradient spin-echo (PGSE) sequence, which replaced Carr and Purcell's constant magnetic field with short duration gradient pulses as illustrated in Figure 1.6. This allowed a clear distinction between the encoding time (pulse duration, δ) and the diffusion time (separation of the two pulses, Δ). A particularly interesting case of this pulse sequence that makes the problem considerably

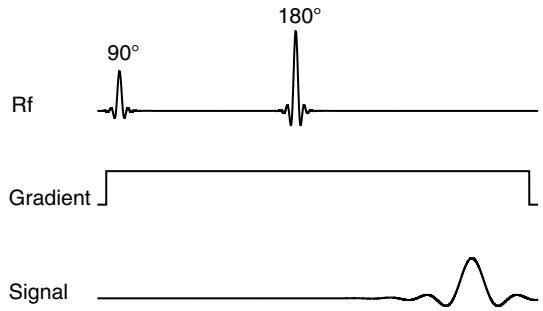

FIGURE 1.5 A schematic of the spin-echo experiment in the presence of a constant field gradient discussed by Carr and Purcell. Diffusion taking place in the resulting inhomogeneous field gives rise to a decreased MR signal intensity.

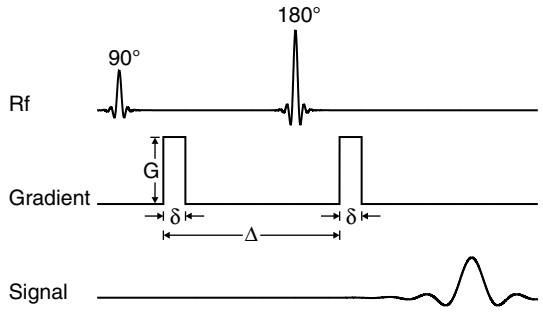

FIGURE 1.6 A schematic of the pulsed field gradient spin-echo MR technique introduced by Stejskal and Tanner. The time between the application of the two gradient pulses, Δ, may be anywhere between 10ms and a few hundreds of milliseconds. The gradient pulse duration, δ, can vary between a few milliseconds to Δ, where when $\delta = \Delta$, the pulse sequence becomes the same as that in Figure 1.5.

simpler – from a theoretical point of view is obtained when the diffusion gradients are so short that diffusion taking place during the application of these pulses can be neglected. In this "narrow pulse" regime, the net phase change induced by the first gradient pulse is given simply by

$$\phi_1 = -q\,x_1 \tag{1.5}$$

where x_1 is the position of the particle during the application of the first pulse and we ignore the phase change due to the B_0 field, which is constant for all spins in the ensemble. In the above expression all experimental parameters were combined in the quantity $q = \gamma\delta G$, where δ and G are the duration and the magnitude of the gradient pulses, respectively. Similarly, if the particle is situated at position x_2 during the application of the second pulse, the net phase change due to the second pulse is given by

$$\phi_2 = -q\,x_2 \tag{1.6}$$

The 180 degree rf pulse applied in between the two gradient pulses reverses the phase change that occurs prior to it, i.e. that induced by the first gradient pulse. Therefore, the aggregate phase change that the particle suffers is given by

$$\phi_2 - \phi_1 = -q(x_2 - x_1) \tag{1.7}$$

Clearly, if particles remained stationary, i.e. $x_1 = x_2$, the net phase shift would vanish. In this case, and in the case in which all spins are displaced by the same constant amount, the magnitude of the echo will be unchanged (except for the T1 and T2 decay that is occurring throughout the sequence). However, if particles diffuse randomly throughout the excited volume, the phase increment they gain during the first period does not generally cancel the phase decrement they accrue during the second period. This incomplete cancellation results in phase dispersion or a spreading of phases among the randomly moving population of spins. Therefore, the overall signal, given by the sum of the magnetic moments of all spins, is attenuated due to the incoherence in the orientations of individual magnetic moments.

It is more convenient to introduce a new quantity, $E(q)$, called MR signal attenuation, than to deal with the MR signal itself. $E(q)$ is obtained by dividing the diffusion-attenuated signal, $S(q)$, by the signal in the absence of any gradients, $S_0 = S(0)$, i.e. $E(q) = S(q)/S_0$. Since relaxation-related signal attenuation is approximately independent of the applied diffusion gradients, dividing $S(q)$ by S_0 eliminates the effects of relaxation, and the q-dependence of $E(q)$ can be attributed solely to diffusion. The MR signal attenuation is then given by

$$E(q) = \int \rho(x_1) \int P(x_1, x_2, \Delta)\, e^{-iq(x_2 - x_1)}\, \mathrm{d}x_2\, \mathrm{d}x_1 \tag{1.8}$$

where we employed two new quantities. The first of these, $\rho(x_1)$, is the spin density at the time of application of the first pulse quantifying the likelihood of finding a spin at location x_1. In most applications, this function can be taken to be a constant throughout the water-filled region, where the value of the constant is determined by setting the integral of $\rho(x_1)$ equal to unity. The second function that we used, $P(x_1, x_2, \Delta)$, is the diffusion propagator (Green's function) that denotes the likelihood that a particle initially located at position x_1 will have ended up at x_2 after a time Δ – the separation of the two gradients. These two functions are related through the expression

$$\lim_{t\to\infty} P(x_1, x_2, t) = \rho(x_1) \tag{1.9}$$

as when the diffusion time is very long, a spin can traverse to any location in space with the same probability. The remaining quantity in equation (1.8),

$$e^{-iq(x_2 - x_1)} = \cos(q(x_2 - x_1)) - i\sin(q(x_2 - x_1)) \tag{1.10}$$

where $i^2 = -1$, is the "Fourier kernel" that is used, e.g., in obtaining the frequency response of a time-dependent signal. Here, the real (cosine) and imaginary (sine) components of the Fourier kernel represent, respectively, the x and y components of the two-dimensional magnetization vector on the plane perpendicular to the main magnetic field, and the integration represents the summation over all possible displacements in the ensemble.

If diffusion is free, the propagator is Gaussian and the MR signal attenuation is given by another Gaussian, $E(q) = e^{-q^2 D\Delta}$. This expression is a special case of the more general Stejskal–Tanner relation, which takes the duration of the pulses into consideration as well, given by

$$\begin{aligned} E(q) &= e^{-q^2 D(\Delta - \delta/3)} \\ &= e^{-bD} \end{aligned} \tag{1.11}$$

where $b = q^2(\Delta - \delta/3) = (\gamma\delta G)^2(\Delta - \delta/3)$ is the b-value discussed above.

Stejskal employed the above formalism for the case of free, anisotropic diffusion in the principal frame of reference (Stejskal, 1965), where he used a "tensor", i.e. a 3×3 matrix that represents the natural orientation of anisotropic diffusion with respect to the three axes of the laboratory reference frame, which is determined by the

orthogonal orientations of the magnetic field gradients produced by the three gradient coils. A general scheme, called diffusion tensor imaging (DTI), was developed to measure the entire diffusion tensor (both its diagonal and off-diagonal elements) in each voxel within the laboratory frame of reference (Basser *et al.*, 1994).

A. From the MR Signal Attenuation to the Average Propagator

To glean the microstructural features of the specimen from the MR signal intensity, one may fit mathematical models to the acquired diffusion-weighted data. However, when the specimen's microstructural features are not known *a priori*, or when the specimen exhibits considerable regional variability like in most applications of biological and medical imaging, an alternative approach that does not assume any particular model may be advantageous. For example, in the above discussion we have not employed any particular model and it would be desirable to obtain the local propagator, $P(x_1, x_2, \Delta)$, employed in equation (1.8) from the MR signal. However, finite resolution of the images and the unavailability of the spin density function prohibit the inference of the local propagator directly from the MR signal.

The difficulty associated with obtaining the local propagator can be overcome to some extent by introducing a net displacement variable $x = x_2 - x_1$ that makes it possible to write the simplified expression

$$E(q) = \int \overline{P}(x, \Delta) e^{-iqx} \, \mathrm{d}x \tag{1.12}$$

where $\overline{P}(x, \Delta)$ is the ensemble average propagator given by

$$\overline{P}(x, \Delta) = \int \rho(x_1) \, P(x_1, x_1 + x, \Delta) \mathrm{d}x_1 \tag{1.13}$$

This procedure, initially proposed by Stejskal (1965), makes it possible to obtain an average propagator from the $E(q)$ data by inverting the Fourier transform in equation (1.12). The propagator reconstructed in this fashion can be envisioned to be a "q-space image" of the displacements (Callaghan *et al.*, 1990). If the diffusion-sensitizing pulses are embedded into imaging protocols and the average propagator is reconstructed at each voxel of the image, spatially localized displacement maps can be obtained (Callaghan *et al.*, 1988); this approach laid the foundation for developments of q-space NMR and MRI (Callaghan, 1991) or equivalently, diffusion spectrum imaging (DSI) (Tuch *et al.*, 2001; Wedeen *et al.*, 2005). The q-space imaging and DSI will be discussed in more detail in Chapters 4 and 7.

III. DIFFUSION IN NEURAL TISSUE

The incessant random motion of water molecules within the tissue is influenced by a variety of factors such as restrictions due to cell membranes, cytoskeleton, and macromolecules (Tanner and Stejskal, 1968). Figure 1.7 depicts how the cells may hinder the otherwise free motion of molecules. By employing the understanding of how microstructural features contribute to the overall diffusional process, it may be possible to obtain valuable information about the biological microstructure simply by observing the motion of water molecules. This is particularly important in the understanding of neural tissue for its notoriously complicated structure.

Enhancing diffusive attenuation with the application of gradients, as we discussed for the case of spin echoes above, introduces a contrast mechanism different

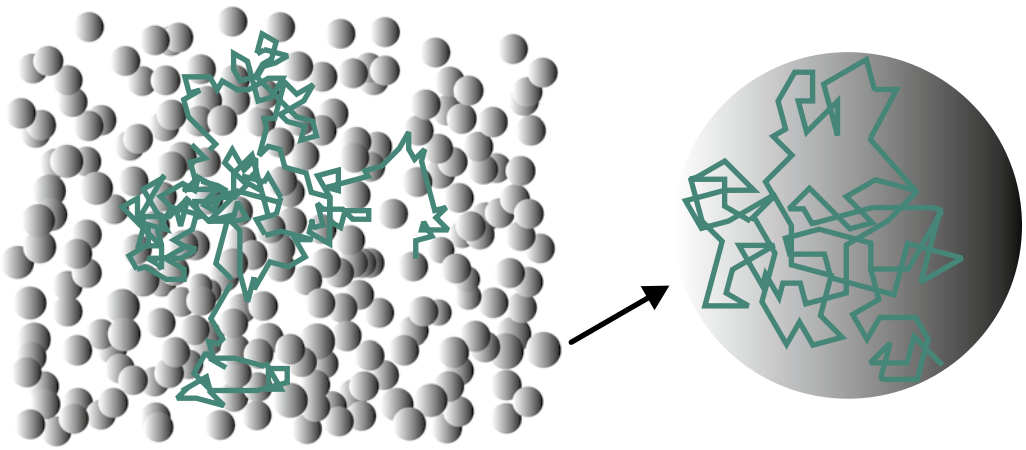

FIGURE 1.7 Biological cells may hinder the Brownian motion of extracellular water molecules (left). Inside each cell, diffusion may be envisioned to be restricted by the cellular membranes (right).

than that in relaxation-weighted magnetic resonance images. Such maps of the signal intensity S are called diffusion-weighted images. Diffusion-weighted images have been utilized extensively in neuroimaging since it was shown that ischemic strokes can be detected much earlier with diffusion-weighted images when compared to traditional T1 and T2 weighted magnetic resonance images (Moseley *et al.*, 1990b). This discovery has made diffusion-weighted imaging an indispensable tool in the diagnosis and management of ischemic stroke.

The central nervous system (CNS) comprises neuronal cells connected to each other through axons that function as transmission lines between different regions. An understanding of how the brain and the spinal cord function is not possible without the knowledge of how different anatomical regions are connected to each other. Since water molecules tend to diffuse more freely along the direction of the fiber, if one can quantify the orientational preference of diffusion, it may be possible to relate it to the axonal orientations.

In tissues, such as brain gray matter, where the measured apparent diffusivity is largely independent of the orientation of the tissue (i.e. isotropic) at the voxel length scale, it is usually sufficient to describe the diffusion characteristics with a single (scalar) apparent diffusion coefficient (ADC). However, in anisotropic media, such as white matter (Henkelman *et al.*, 1994; Moseley *et al.*, 1990a, 1991) or skeletal and cardiac muscle (Cleveland *et al.*, 1976; Garrido *et al.*, 1994; Tanner, 1979), where the measured diffusivity is known to depend upon the orientation of the tissue, a single ADC does not adequately characterize the orientation-dependent water mobility. The next most complex model that describes anisotropic diffusion replaces the scalar ADC with a symmetric effective or apparent diffusion tensor of water, **D** (e.g. see Crank, 1975).

The causes or biophysical basis of diffusion anisotropy in brain parenchyma and other tissues have not been fully elucidated, although most investigators ascribe it to ordered, heterogeneous structures, such as large oriented extracellular and intracellular macromolecules, supermacromolecular structures, organelles, and membranes. Clearly, in the central nervous system (CNS), diffusion anisotropy in white matter is not simply caused by myelin, since several studies have shown that even before myelin is deposited, diffusion anisotropy can be measured using MRI (Neil *et al.*, 1998; Beaulieu and Allen, 1994a, b; Wimberger *et al.*, 1995). Thus, despite the fact that increases in myelin are temporally correlated with increases in diffusion anisotropy, structures other than the myelin sheath must significantly contribute to diffusion anisotropy (LeBihan *et al.*, 1993). This is important because the degree of diffusion anisotropy is not a quantitative measure or "stain" of myelin content (Pierpaoli and Basser, 1996). The anatomical determinants of diffusion anisotropy will be discussed in great detail in Chapter 5.

IV. CONCLUDING REMARKS

As water (or another spin-labeled molecule) undergoes diffusion, it also encounters barriers, macromolecules, sampling many different local environments. Collectively, the signal we measure in an MR experiment contains contributions from water motion in these various microenvironments. The challenge in diffusion NMR and MRI is to try to infer features of the local tissue anatomy, composition, and microstructure from MR displacement measurements. One great advantage of MR is that it permits one to probe tissue structure at different length scales (Özarslan and Basser, 2008) – i.e. levels of hierarchical architectural organization (Özarslan *et al.*, 2006). Specifically, while the mean-squared displacement of water is on the order of microns for typical MR experiments, these molecular motions are ensemble-averaged within a voxel, and then subsequently assembled into multislice or 3D images of tissues and organs. Thus, this imaging modality permits us to study and elucidate complex structural features spanning length scales ranging from the macromolecular to the macroscopic – without the use of exogenous contrast agents.

ACKNOWLEDGMENTS

This research was supported by the Intramural Research Program of the Eunice Kennedy Shriver National Institute of Child Health and Human Development.

REFERENCES

Abragam A (1961) *The Principles of Nuclear Magnetism*. Oxford: Clarendon Press.

Basser PJ, Mattiello J, LeBihan D (1994) Estimation of the effective self-diffusion tensor from the NMR spin echo. *J Magn Reson B* 103(3):247–254.

Beaulieu C, Allen PS (1994a) Determinants of anisotropic water diffusion in nerves. *Magn Reson Med* 31(4):394–400.

Beaulieu C, Allen PS (1994b) Water diffusion in the giant axon of the squid: implications for diffusion-weighted MRI of the nervous system. *Magn Reson Med* 32(5):579–583.

Berg HC (ed.) (1983) *Random Walks in Biology*. Princeton, NJ: Princeton University Press.

Bloch F (1946) Nuclear induction. *Phys Rev* 70(7,8):460–474.

Brown R (1828) A brief account of microscopical observations made in the months of June, July, and August, 1827, on the particles contained in the pollen of plants; and on the general existence of active molecules in organic and inorganic bodies. *Phil Mag* 4:161–173.

Callaghan PT (1991) *Principles of Nuclear Magnetic Resonance Microscopy*. Oxford: Clarendon Press.

Callaghan PT, Eccles CD, Xia Y (1988) NMR microscopy of dynamic displacements: **k**-space and **q**-space imaging. *J Phys E* 21:820–822.

Callaghan PT, MacGowan D, Packer KJ, Zelaya FO (1990) High-resolution *q*-space imaging in porous structures. *J Magn Reson* 90:177–182.

Carr HY, Purcell EM (1954) Effects of diffusion on free precession in nuclear magnetic resonance experiments. *Phys Rev* 94(3):630–638.

Chandrasekhar S (1943) Stochastic problems in physics and astronomy. *Rev Mod Phys* 15(1):1–89.

Cleveland GG, Chang DC, Hazlewood CF, Rorschach HE (1976) Nuclear magnetic resonance measurement of skeletal muscle: anisotropy of the diffusion coefficient of the intracellular water. *Biophys J* 16(9):1043–1053.

Crank J (1975) *Mathematics of Diffusion*. Oxford: Clarendon Press.

Einstein A (1905) Über die von der molekularkinetischen Theorie der wärme gefordete Bewegung von in ruhenden Flüssigkeiten suspendierten Teilchen. *Ann Physik* 4:549–560.

Einstein A (1926) *Investigations on the Theory of the Brownian Movement*. New York: Dover Publications, Inc.

Fick A (1855a) Concerns diffusion and concentration gradient. *Ann Phys Lpz* 170:59.

Fick A (1855b) Über diffusion. *Ann Phys* 94:59.

Fürth R, Cowper AD (eds) (1956) *Investigations on the Theory of the Brownian Movement*. New York: Dover Publications.

Garrido L, Wedeen VJ, Kwong KK, Spencer UM, Kantor HL (1994) Anisotropy of water diffusion in the myocardium of the rat. *Circ Res* 74(5):789–793.

Hahn EL (1950) Spin echoes. *Phys Rev* 80:580–594.

Henkelman RM, Stanisz GJ, Kim JK, Bronskill MJ (1994) Anisotropy of NMR properties of tissues. *Magn Reson Med* 32:592–601.

LeBihan D, Turner R, Douek P (1993) Is water diffusion restricted in human brain white matter? An echo-planar NMR imaging study. *Neuroreport* 4(7):887–890.

Moseley ME, Cohen Y, Kucharczyk J, Mintorovitch J, Asgari HS, Wendland MF, Tsuruda J, Norman D (1990a) Diffusion-weighted MR imaging of anisotropic water diffusion in cat central nervous system. *Radiology* 176(2):439–445.

Moseley ME, Cohen Y, Mintorovitch J, Chileuitt L, Shimizu H, Kucharczyk J, Wendland MF, Weinstein PR (1990b) Early detection of regional cerebral ischemia in cats: comparison of diffusion and T_2-weighted MRI and spectroscopy. *Magn Reson Med* 14:330–346.

Moseley ME, Kucharczyk J, Asgari HS, Norman D (1991) Anisotropy in diffusion-weighted MRI. *Magn Reson Med* 19(2):321–326.

Neil JJ, Shiran SI, McKinstry RC, Schefft GL, Snyder AZ, Almli CR, Akbudak E, Aronovitz JA, Miller JP, Lee BC, Conturo TE (1998) Normal brain in human newborns: apparent diffusion coefficient and diffusion anisotropy measured by using diffusion tensor MR imaging. *Radiology* 209(1):57–66.

Özarslan E, Basser PJ (2008) Microscopic anisotropy revealed by NMR double pulsed field gradient experiments with arbitrary timing parameters. *J Chem Phys* 128(15):154511.

Özarslan E, Basser PJ, Shepherd TM, Thelwall PE, Vemuri BC, Blackband SJ (2006) Observation of anomalous diffusion in excised tissue by characterizing the diffusion-time dependence of the MR signal. *J Magn Reson* 183(2):315–323.

Pierpaoli C, Basser PJ (1996) Toward a quantitative assessment of diffusion anisotropy. *Magn Reson Med* 36(6):893–906.

Smoluchowski MR (1906) Zur kinetischen Theorie der Brownschen Molekularbewegung und der Suspensionen. *Ann Phys* 21:756–780.

Stejskal EO (1965) Use of spin echoes in a pulsed magnetic-field gradient to study anisotropic, restricted diffusion and flow. *J Chem Phys* 43(10):3597–3603.

Stejskal EO, Tanner JE (1965) Spin diffusion measurements: spin echoes in the presence of a time-dependent field gradient. *J Chem Phys* 42(1):288–292.

Tanner JE (1979) Self diffusion of water in frog muscle. *Biophys J* 28(1):107–116.

Tanner JE, Stejskal EO (1968) Restricted self-diffusion of protons in colloidal systems by the pulsed-gradient, spin-echo method. *J Chem Phys* 49(4):1768–1777.

Torrey HC (1956) Bloch equations with diffusion terms. *Phys Rev* 104(3):563–565.

Tuch DS, Wiegell MR, Reese TG, Belliveau JW, Wedeen VJ (2001) Measuring cortico-cortical connectivity matrices with diffusion spectrum imaging. In: *Proc. of the 9th Annual Meeting of ISMRM*, Glasgow, p. 502.

Wedeen VJ, Hagmann P, Tseng W-YI, Reese TG, Weisskoff RM (2005) Mapping complex tissue architecture with diffusion spectrum magnetic resonance imaging. *Magn Reson Med* 54(6):1377–1386.

Wimberger DM, Roberts TP, Barkovich AJ, Prayer LM, Moseley ME, Kucharczyk J (1995) Identification of "premyelination" by diffusion-weighted MRI. *J Comput Assist Tomogr* 19(1):28–33.